

Second-Harmonic Generation in SiO₂ - GeO₂ Waveguides

Ulf Österberg

Thayer School of Engineering

Dartmouth College

Hanover, N.H. 03755

USA

ABSTRACT

We discuss the microscopic origin of second-harmonic generation in glasses. All models presented to date to explain second-harmonic generation in optical fibers rely on interactions between different types of defects and the intense laser light. The most common description for the interaction is through an internally generated dc-field. Other descriptions involve van der Waals forces and direct laser induced orientation of defects. A possible mechanism for saturation will also be considered.

I. INTRODUCTION

The discovery of efficient second-harmonic generation (SHG) in optical glass fibers was very surprising [1], since glass is amorphous and therefore should not exhibit any second-order nonlinear phenomena [2]. It turns out that the SH signal does not reach its maximum value immediately; instead, it grows several orders of magnitude during a period of time that can vary from 1/2 - 10 hours, depending on the experimental conditions. The best conversion efficiency obtained in commercially available optical fibers is 5% with an input peak power of 20 kW at $\lambda=1.06 \mu\text{m}$ [3]. In specially prepared fibers 13% conversion efficiency has been obtained with only 950 W input peak power [4]. In such optical fibers, frequency-doubling has been efficient enough to pump dye-lasers [5] and autocorrelate picosecond-pulses [6].

Even though these conversion efficiencies for optical fibers are impressive, they are still far from competitive for frequency-doubling semiconductor lasers compared to waveguides in LiNbO_3 [7] and KTP [8]. We believe therefore, that the most important outcome of the research on SHG in optical fibers will not be a commercial device using a fiber, but understanding the underlying physical mechanism to see if that can be used to improve the frequency-doubling efficiency in other materials. For example, one of the few things that is widely agreed to occur in an optical fiber during preparation is the inducement of a periodic structure [9,10]. This periodic structure is believed to be instrumental in achieving phase-matching between the fundamental and harmonic light. In an optical fiber this so called quasi-phases-matching [11] occurs spontaneously, in contrast to materials such as LiNbO_3 where elaborate fabrication techniques have to be utilized. It is therefore of interest to determine if special dopants in ferroelectric materials would make them susceptible to the same type of photoinduced changes that occur in optical glass fibers.

To give a comprehensive picture of the physics behind SHG in optical waveguides, we start by describing some macroscopical phenomenological models, thereafter we

discuss what types of defects or molecules in general could be involved. In both these sections we will use experimental data to argue for and against various models.

II. PHENOMENOLOGICAL MODELS

Any model attempting to explain SHG in optical glass fibers has to address, at least, the following two experimental observations:

1. High conversion efficiency
2. SH light is coherent

The first point is obviously crucial since optical fibers do not intrinsically possess a large second-order nonlinearity. The second point is important because it proves that the SH light in an optical fiber is due to a coherent nonlinear process and not just from luminescence.

In the following section we will describe a few of the models that have been put forward to date to explain SHG in optical glass fibers. To better understand these models, we will begin by giving a short introduction to electric field-induced second-harmonic generation.

A. Electric field-induced second-harmonic generation

Electric field-induced second-harmonic generation (EFISH) is a well-known technique for producing SH light in a medium which is centrosymmetric. EFISH is a third-order nonlinear interaction in which an electric dc-field interacts with two photons at the fundamental frequency to produce one photon at the second-harmonic frequency.

$$\omega + \omega + 0 \rightarrow 2\omega \quad (1)$$

In the notation of nonlinear susceptibilities, we can represent EFISH in terms of an effective second-order susceptibility

$$\chi_{\text{eff}}^{(2)} = 3 \cdot \chi^{(3)} \cdot E^{\text{DC}} \quad (2)$$

E^{DC} is, in most cases, an externally generated dc-field [12,13].

An additional advantage with EFISH is that when used on centrosymmetric media such as gases and liquids that can have coherence lengths in the order of centimeters, the externally applied field can be alternated, thereby producing phasematching. The explanation for this is that the dc-field aligns either existing or induced dipoles so as to break the inversion symmetry and create an effective $\chi^{(2)}$ (eq. 2). If then the coherence length is on the order of a few centimeters, one can easily fabricate electrodes with alternating polarity creating an effective $\chi^{(2)}$ according to eq. 3:

$$\chi_{\text{eff}}^{(2)} = \chi_0^{(2)} \cos \Lambda z = \frac{1}{2} \chi_0^{(2)} [e^{i\Lambda z} + e^{-i\Lambda z}] \quad (3)$$

with Λ being the spatial periodicity for the electrodes. If the above $\chi_{\text{eff}}^{(2)}$ is inserted into the well-known equations for SHG [14], we obtain

$$\frac{dE_{\omega}}{dz} = i\kappa \chi_{\text{eff}}^{(2)} E_{\omega}^* E_{2\omega} e^{i\Delta\beta z} \quad (4a)$$

$$\frac{dE_{2\omega}}{dz} = i\kappa \chi_{\text{eff}}^{(2)} E_{\omega}^2 e^{-i\Delta\beta z} \quad (4b)$$

where $\kappa = \frac{\mu_0 \epsilon_0 \omega}{2n}$ and $\Delta\beta = \beta_{2\omega} - 2\beta_{\omega}$ is the phasemismatch. Inspection of (3) and (4)

shows that phasematching can be obtained if the distance between the electrodes are chosen so that

$$\Lambda = \Delta\beta \quad (5)$$

The above two properties of EFISH, namely i) creating an effective second-order nonlinear susceptibility in a medium with inversion symmetry, and ii) having the potential for producing perfect phasematching, are essential for most of the macroscopic models presented to date to explain SHG in optical fibers. The difficulty with the optical fibers is to explain the origin of a light-induced electric dc-field in the glass.

B. Light-induced electric dc-fields in glass

The first model to discuss the possibility of an internally generated dc-field in the glass was suggested by Stolen & Tom [15]. They proposed that fundamental and harmonic light could mix via a $\chi^{(3)}$ process to produce a dc-field

$$E^{DC} = \frac{3\pi}{\epsilon} | \chi^{(3)} E_{\omega}^2 E_{2\omega}^* | \cdot \cos \Delta\beta z \quad (6)$$

which through EFISH would give the SH light. From eq. 6 it is seen that their electric dc-field will be oscillating with just the right periodicity to also give a phasematched process.

The first experiments on SHG in optical fibers were done by sending intense ($\sim 1 - 100 \text{ GW/cm}^2$) laser light at the fundamental frequency down a $\sim 1\text{m}$ long fiber. Over a period of several hours, the SH light could be seen to grow until it saturated. In these experiments, the initial amount of green light was of the order of 10^{-12} W average power. An obvious test for the Stolen & Tom model was to use externally generated harmonic light together with the fundamental light during the preparation process. This experiment was performed [15] and the preparation time was reduced from several hours to $\sim 1/2$ hour, in excellent agreement with their predictions. There is, however, one major difficulty with this model and that is the magnitude of the electric dc-field. It is only $1\text{mV} - 1\text{V/cm}$ for the light intensities involved [16,17]. To get an appreciation of how small this number is: if $E^{DC} = 100 \text{ kV/cm}$, $\mu = 1\text{D}$ and $T = 300\text{K}$, we obtain $\mu E^{DC} \sim 0.01 \text{ kT}$. Effects of this field might therefore be expected to be averaged out by thermal effects.

The second model to discuss an internally generated electric dc-field was proposed by Lawandy [18]. In this model it is assumed that defects present in the glass produce midgap states in the $\text{SiO}_2 : \text{GeO}_2$ band gap [19]. At first these midgap states are localized, but as the glass is irradiated with intense nonresonant laser light, the energy levels for these midgap states are shifted so that for a critical power we get a transition from localized to extended states.

A consequence of the transition to extended states is that carrier diffusion is dramatically facilitated leading to a carrier density gradient in the glass. This displacement of charges can then lead to an electric dc-field

$$E^{DC} = \frac{2\rho_0 d e}{\epsilon_r \epsilon_0} \quad (7)$$

where ρ_0 is the defect density, d is the fiber mode intensity width at half maximum, and the other parameters have their usual meaning. For typical values ($\rho_0 \sim 5 \times 10^{13} / \text{cm}^3$ and $d \sim 2 \mu\text{m}$) it is predicted that in glass $E^{DC} \sim 10^4 \text{ V/cm}$.

A third model concerned with a dc-field picture was proposed by Anderson [20]. Again, energy levels are assumed to be present in the glass bandgap due to defects, but these levels are closer to the conduction and valence bands and referred to as donors and acceptors. As the fiber is illuminated, these defect states are assumed to be ionized and when recombined a charge carrier has a certain probability of being displaced from its original site. This, then, leads to transport of carriers within the glass. Since the laser light propagates in a Gaussian-like mode, there will be more charges ionized in the center of the fiber than at the core-cladding leading to a charge gradient density setting up a radial electric field

$$E^{DC} = -\frac{kT}{e} \frac{\nabla I}{I} \quad (8)$$

This field has been predicted to be in the order of 1 - 10 kV/cm (see fig. 1).

The last electric dc-field model we will discuss is proposed by Dianov et al [21]. In this model, a photocurrent j_{ph} is proposed to occur from a third-order nonlinear interaction between the fundamental and harmonic lights. As the fiber is illuminated, this photocurrent will force photoelectrons (excited from defects) to drift into regions that are not exposed to light. This will then give rise to an electrostatic space charge field

$$E^{DC} = \frac{j_{ph}}{\sigma} \quad (9)$$

where σ is the photoconductivity. For a photoconductivity of $\sim 10^{-10}/\Omega$ cm and typical light intensities, this model also predicts a $E^{DC} \sim 10$ kV/cm.

It should be mentioned that for these last three models, phasematching is also obtained through a spatially varying electric dc-field. In these models, it comes about through the spatial variation of light intensities along the fiber. Furthermore, the last three models rely on the presence of an electric dc-field but not necessarily the alignment of dipoles as discussed by Stolen & Tom [15].

C. Light-induced polarization of dipoles

The very first model to attempt to explain SHG in optical fibers was proposed by Farries et al [22]. They assumed the orientation of dipole centers by the polarized light itself and that these dipole centers were formed by the interaction of the harmonic light with the dopants in the glass. Since the intensity of the intrinsically generated harmonic light is periodic along the fiber due to the inherent phasemismatch, the aligned dipoles will have the right periodicity for phasematching the photoinduced harmonic light.

D. Dipole – dipole interactions

The last model we present is based upon van der Waals interactions between dipoles in the glass matrix [23]. The assumption is that there are defects in the glass which have a non-zero second-order polarizability; however, due to the randomness of the glass, the macroscopic susceptibility averages out to zero. The idea is that the presence of light at the harmonic frequency will cause these defects to interact. Since the light is polarized, there will be a preferred direction leading to a non-zero macroscopic second-order susceptibility.

E. Discussion of macroscopic models

Based upon temperature and polarization measurements, we will make some comments on the above briefly described models.

There have been four temperature measurements reported in the literature so far [21, 24-26]. The first temperature measurements [21,24] were made on prepared fibers for which the conversion efficiency was recorded for $295 \text{ K} < T < 573 \text{ K}$ in one case [21] and $295 \text{ K} < T < 673 \text{ K}$ for the other case [24]. In both these experiments, it was shown that the efficiency dropped a factor of 10 when the temperature was increased. These experiments cast little light on which of the models might be correct, but are of interest in determining what kind of defects could be involved (see next section).

The other two measurements [25,26] both deal with the growth rate and conversion efficiency for fibers that are being prepared at either liquid nitrogen temperature (LT) or room temperature (RT). One measurement [25] showed no difference between fibers that had been prepared at LT compared to RT, while the other measurement [26] showed a faster growth rate and 20 times larger conversion efficiency for fibers prepared at RT compared to LT. If the latter experiment is correct, any model which uses alignment of dipoles, with or without an electric dc-field, would be highly dubious. However, a charge migration model like the Anderson model could possibly have the kind of temperature dependence measured in ref. 26.

It is unfortunate that there are contradictory experimental results. This, however, is common in the field of SHG in optical fibers, possibly because there are so many different experimental variables to be controlled.

Another important experiment where contradictory results also have been reported is the polarization properties of the induced SH light [27,28]. For the geometry of the polarization measurements we refer to figure 2. In ref. 27 the fibers were prepared with fundamental and harmonic (externally generated) light both polarized in the x-direction. From this measurement, it was concluded that $\chi_{xxx}^{(2)}/\chi_{yxx}^{(2)} \sim 0.008$, in good agreement with a picture of an electric dc-field induced $\chi^{(2)}$. As was pointed out in ref. 27, this does not necessarily mean that dipoles have to be aligned in this field.

The second experiment [28] was done by preparing the fibers with only fundamental light (in the x-direction). In this case, electric quadrupole interactions at the core-cladding interface are responsible for the initial harmonic light [29]. Here it was shown that the initial intensity ratio between harmonic light in the x- and y-direction, for both fundamental photons in the x-direction, is ~ 0.3 . As the harmonic light grows, this ratio was seen to decrease to $\chi_{xxx}^{(2)}/\chi_{yxx}^{(2)} \sim 0.2$. This is a rather remarkable finding since it shows that the harmonic light perpendicular to the preparation polarization grows almost seven orders of magnitude. This result is very different from ref. 27 and does not lend itself to an electric dc-field model in the fiber unless we require this field to be of a very complex form. However, contrary to the temperature measurements, the two sets of polarization measurements were done under very different experimental conditions. In ref. 27, the harmonic light used in the preparation stage was six orders of magnitude stronger than in the experiment of ref. 28. Furthermore, in ref. 28 the two perpendicular directions of the harmonic light started off with a ratio of 3:1, while in ref. 27 this ratio was $10^6:1$.

Since these two polarization measurements were made, an experiment has been performed that measured an intrinsic dc-field of ~ 10 kV/cm in the fiber [30]. From earlier measurements, it is not clear whether 10 kV/cm is enough to induce a permanent $\chi^{(2)}$ in the glass [16], but it is, nevertheless, very interesting that an electric dc-field exists in a prepared fiber.

III. DEFECTS

In all of the models described earlier, it has tacitly been assumed that the glass fiber contains some sort of defect with which the intense laser light interacts to modify the properties of the glass.

Since most of the fibers used for SHG are based upon SiO_2 with a few molar percent of GeO_2 in the core, it was suggested early on that the so-called GeE' defects could

be responsible for the alterations in the glass [31]. One GeE' defect out of four possible is depicted in fig. 3. The defect can, for instance, be generated by breaking the bond between the Ge and Si atoms with two photons from the harmonic light.

In a correlation study using electron spin resonance (ESR) [33], it was found that an increase of photogenerated GeE' defects was related to an increase of SHG. It was also observed in the same study that GeE' defects produced during the fabrication process did not participate in the SHG process.

Another observation supporting the involvement of GeE' defects in the SHG process is the experiment of Fermann [24] demonstrating that the SHG can be annealed out of the fiber. This type of temperature sensitivity is what one would expect from a paramagnetic defect such as the GeE'.

A word of caution is, however, appropriate at this point. The correlation study mentioned above used only ESR to study the fiber before and after preparation. ESR detects only defects with an unpaired spin, and other (possibly more important) changes in the glass might have escaped unnoticed.

One experimental observation made by several groups [34-36] is that fibers with small percentage of P₂O₅ added to them (in addition to the GeO₂) reach by far the highest conversion efficiencies of SHG. No phosphorous-related defects have been found in prepared fibers [33]. It has been speculated that the role of phosphorous is to limit saturation mechanisms in the glass [36].

In trying to understand the physics of the defects involved in the SHG process, bleaching experiments have been performed [37,38]. It was found that whatever alterations were made to the glass during preparation could be erased by exposing the fiber to light at 532 nm or shorter. The erasure time was found to be similar to the preparation time. If we, in analogy with most of the models presented earlier, assume a photoinduced $\chi^{(2)}$ grating with an amplitude A, the experiments of ref. 37, 38 show that A grows and decays according to the following relations:

$$\frac{dA}{dt} \propto \sqrt{I_{2\omega}} \quad (10)$$

$$\frac{dA}{dt} \propto -I_{\text{erasure}}^4 \cdot A^2 \quad (11)$$

where I_{erasure} is the intensity of the light used to bleach the photoinduced defects.

Equations (10) and (11) are fits to experimental data and are at a first glance contradictory. Equation (10) indicates that the growth of the induced $\chi^{(2)}$ amplitude is proportional to the amplitude itself. This is in contrast to equation (11) where the decay rate of the $\chi^{(2)}$ amplitude is best fitted to the square of the same amplitude. A square dependency would mean that the defects are interacting with each other.

The concept of interacting defects is interesting and we will discuss it in slightly more detail. In fig. 4, we have depicted a generic charge distribution $\rho(\mathbf{r})$ around a Germanium-Silicon-Oxygen complex in the glass network. If the electromagnetic field of the incoming light is strong enough to break the bond between the Ge-Si atoms, we will locally distort the charge distribution and possibly produce a charge separation around the created defect (see fig. 4). This induced dipole could then interact with similarly induced dipoles very much the same way suggested by Dianov et al (see Section II).

This interaction that depends inversely on the distance between the fluctuating dipoles to the power six would lead very small local perturbations to drastically alter the macroscopic properties of the glass. If in the interaction between the defect charge distributions higher-order multipole moments are incorporated, it is possible to account for the large growth of perpendicular harmonic light [39].

To end the section on defects, we would like to emphasize the importance of obtaining more spectroscopic data on the glasses used for SHG. In fig. 5 we show three different generic energy diagrams for a germanosilicate glass. Diagram A refers to energy levels that could be generated through processes similar to those that occur when an optical

fiber is irradiated with X-rays. Diagram B is related to the midgap states discussed by Lawandy [18], and diagram C shows the internal energy levels of GeO arbitrarily positioned in the bandgap. Not only for the growth process but also for possible saturation mechanisms it is vital to know where the different energy levels are located. It has been suggested [40] that most of the experimentally observed saturation behaviors could be explained by incorporating two-photon and free-carrier absorption. As long as no information exists about possible energy levels in the SiO₂ bandgap, that hypothesis cannot be tested.

So far, the only experimental evidence of an energy level in the SiO₂ bandgap in a germanium-doped optical glass fiber that has been reported in relation to SHG used the third-harmonic light from the fiber itself as the excitation source [41]. The fluorescent light observed is consistent with an energy level ~ 2.95 eV above the valence band (see fig. 6).

IV. WAVE PROPAGATION

Up to now, we have primarily been concerned with the various physical properties of the glass in conjunction with the growth of the SH signal. There is, however, much to learn about possible models just from studying equations 4a and b.

First of all, if we assume that $\chi_{\text{eff}}^{(2)}$ is a function of the green light, we immediately see from eq. 4b that the seed and induced harmonic light are $\pi/2$ out of phase. This phase shift has been observed [42] for fibers prepared with external seed harmonic light and is a possible source for saturation, limiting the amount of induced harmonic light to the same level as the seed harmonic light. It is interesting to note that in the case of internal seeding due to electric quadrupole interactions, this phase shift does not arise since then $\chi_{\text{eff}}^{(2)} = i \beta_{\omega} \chi_{\text{Q}}^{(2)}$ [14]. Possibly as a consequence of this, the highest conversion efficiencies have been obtained using internal seeding.

For any suggested model, as was pointed out by Anderson [43], it is important that it is self-consistent (see fig. 7). This means, in terms of equation 4b, that as we put a new $\chi^{(2)}$ (from some mechanism) into the equation, it will produce more harmonic light that will give rise to a "larger" $\chi^{(2)}$ that will produce more harmonic light, and so on, as we propagate along the fiber.

A last observation that can be made by some simple numerical modeling of equations 4a and b is that it is necessary to have a periodic $\chi_{\text{eff}}^{(2)}$ with a strong length dependence in order to fit experimental SH growth data. A suitable candidate is

$$\chi_{\text{eff}}^{(2)}(z) = \chi_0^{(2)} \cdot e^{\alpha z} \cdot e^{i\Delta\beta z} \quad (12)$$

Equation (12) is not as farfetched as it might first seem. A simple phenomenological model that could give rise to (12) is to assume that

$$\frac{d\chi_{\text{eff}}^{(2)}}{dz} = \text{const.} \cdot I_{2\omega}(z) \quad (13)$$

Since $I_{2\omega}(z)$ is periodic to begin with, due to the intrinsic phase mismatch, the $\chi_{\text{eff}}^{(2)}$ obtains the right periodicity and its growth rate is proportional to the green light, ensuring exponential growth along the fiber.

V. CONCLUSION

In this paper, we have presented the different models that have been published to explain SHG in glass optical fibers. We have also briefly discussed some of the physical insight that exists about defect formation in germanosilicate fibers. Finally, we have given some examples of what information can be gained from simple manipulations of the wave equation. In conclusion, it seems to us that the main thrust for future experiments in the

field of SHG in optical fibers must be focussed on the microscopic properties of the glasses.

VI. REFERENCES

1. U. Österberg and W. Margulis, IQEC '86 Technical Proceedings, p. 102, San Francisco, June 1986.
2. Y. R. Shen, The principles of nonlinear optics, Wiley-Interscience, New York, 1984.
3. U. Österberg and W. Margulis, *Opt. Lett.* **12**, 57 (1987).
4. M. C. Farries, *Laser Focus* **24** (9), 12 (1988).
5. U. Österberg and W. Margulis, *Opt. Lett.* **11**, 516 (1986).
6. U. Österberg and W. Margulis, *IEEE J. Quant. El.* **QE-24**, 2127 (1988).
7. J. Webjörn, F. Laurell and G. Arvidsson, *Phot. Tech. Lett.* **1**, 316 (1989).
8. C. J. van der Poel, J. D. Bierlein, J. B. Brown and S. Colak, *Appl. Phys. Lett.* **57**, 2074 (1990)
9. H. W. K. Tom, R. H. Stolen, G. D. Aumiller and W. Pleibel, *Opt. Lett.* **13**, 512 (1988).
10. A. Kamal, D. A. Weinberger and W. H. Weber, *Opt. Lett.* **15**, 613 (1990).
11. J. A. Armstrong, N. Bloembergen, J. Ducving and P. S. Pershan, *Phys. Rev.* **127**, 1918 (1962).
12. P. D. Maker and R. W. Terhune, *Phys. Rev.* **137**, 801 (1965).
13. R. Kashyap, *JOSAB* **6**, 313 (1989).
14. P. N. Butcher and D. Cotter, The elements of nonlinear optics, Cambridge University Press, Cambridge, 1990.
15. R. H. Stolen and H. W. K. Tom, *Opt. Lett.* **12**, 585 (1987).
16. V. Mizrahi, U. Österberg, J. E. Sipe and G. I. Stegeman, *Opt. Lett.* **13**, 279 (1988).
17. V. Mizrahi, U. Österberg, C. Krautschik, G. E. Stegeman, J. E. Sipe and T. F. Morse, *Appl. Phys. Lett.* **53**, 557 (1988).
18. N. M. Lawandy, *Proc. SPIE* **1148**, 175 (1989).
19. N. M. Lawandy, *Opt. Comm.* **74**, 180 (1989).
20. D. Z. Anderson, *Proc. SPIE* **1148**, 186 (1989).
21. E. M. Dianov, P. G. Kazansky and D. Yu Stepanov, *Sov. J. Quantum El.* **19**, 575 (1989).

22. M. C. Farries, P. St. Russell, M. E. Fermann and D. N. Payne, *Electronics Lett.* **23**, 322 (1987).
23. E. M. Dianov, A. M. Prokhorov, V. O. Sokolov and V. B. Sulimov, *JETP Lett.* **50**, 13 (1989).
24. M. E. Fermann, Ph.D. Thesis, University of Southampton (1988).
25. M. D. Selker and N. M. Lawandy, *Electronics Lett.* **25**, 1440 (1989).
26. Y. Hibino, V. Mizrahi and G. E. Stegeman, *Electronics Lett.* **26**, 1578 (1990).
27. V. Mizrahi, Y. Hibino and G. I. Stegeman, *Opt. Comm.* **78**, 283 (1990).
28. U. Österberg, R. I. Lawconnell and J. W. Leitch, Relative measurements of tensor components for intrinsic and induced second-order nonlinear susceptibilities in optical fibers, submitted to *Opt. Comm.*
29. U. Österberg, R. I. Lawconnell, L. A. Brambani, C. G. Askins and E. J. Friebele, Modal evolution of induced second-harmonic light in an optical fiber, *Opt. Lett.*, in press.
30. A. Kamal, M. L. Stock, A. Szpak, C. H. Thomas, D. A. Weinberger, M. Frankel, J. Nees, K. Ozaki and J. A. Valdmanis, "Electro-optic sampling measurements of the built-in field in fibers conditioned for second-harmonic generation," Optical Society of America annual meeting, Nov. 4-9, 1990, postdeadline paper 25.
31. L. J. Poyntz-Wright, P. St. J. Russell and M. E. Fermann, *Opt. Lett.* **13**, 1023 (1988).
32. E. J. Friebele and D. L. Griscom, *Proc. Mat. Res. Soc.* **61**, 319 (1986).
33. T. E. Tsai, M. A. Saifi, E. J. Friebele, D. L. Griscom and U. Österberg, *Opt. Lett.* **14**, 1023 (1989).
34. W. Margulis and U. Österberg, *SPIE*, Cannes, France, Nov. 16-20 (1987).
35. M. C. Farries, M. E. Fermann and P. St. J. Russell, Topical meeting on nonlinear guided-wave phenomena: physics and applications, *Techn. Dig. Series 2*, 246 (1989).
36. A. Kamal and D. A. Weinberger, Topical meeting on integrated photonics research, March 26-30, 1990, Hilton Head, South Carolina, paper MJ2.
37. F. Oullette, K. O. Hill and C. D. Johnson, *Opt. Lett.* **13**, 515 (1988).
38. A. Krothus and W. Margulis, *Appl. Phys. Lett.* **52**, 1942 (1988).
39. S. Keilich, *Opto-electronics* **2**, 5 (1970).
40. K. Carlson and U. Österberg, Optical Society of America annual meeting, Nov. 4-9, 1990, paper TuD7.
41. U. Österberg, *Electronics Lett.* **26**, 103 (1990).

42. W. Margulis, I. C. S. Carvalho and J. P. von der Weid, *Opt. Lett.* **14**, 700 (1989).
43. D. Z. Anderson, University of Boulder, private communication.

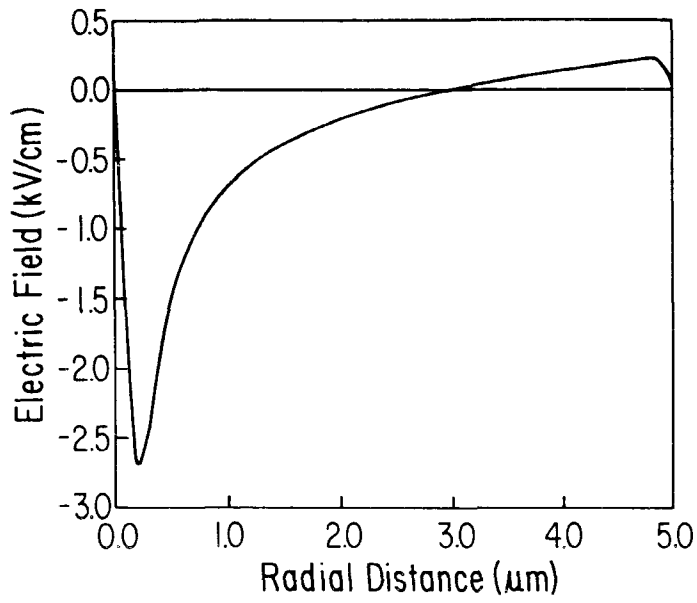


Figure 1 Induced electric dc-field as a function of core-radius in an optical fiber (from ref. 20).

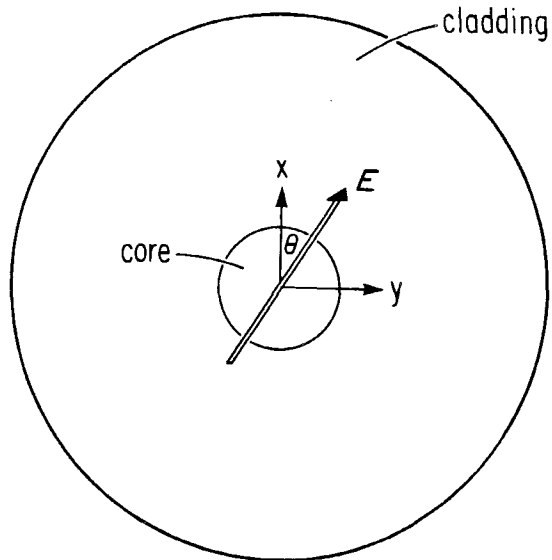


Figure 2 Fiber geometry for polarization measurements

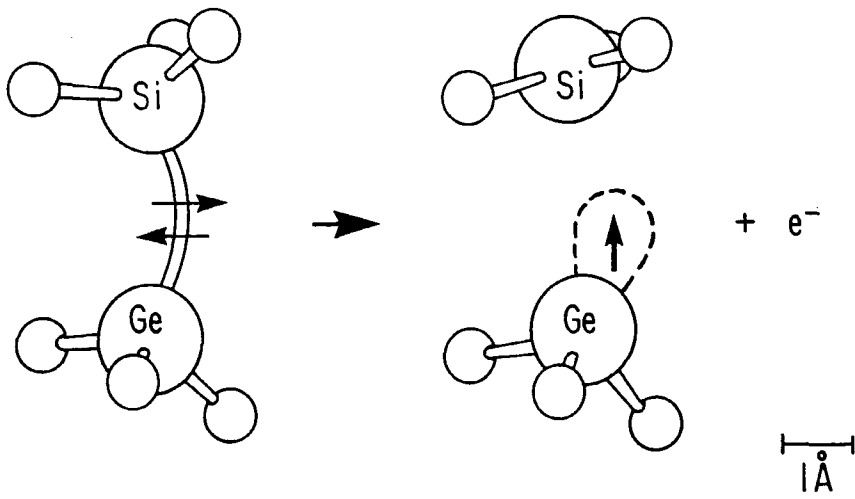


Figure 3 Model of the Ge E' center (from ref. 32)

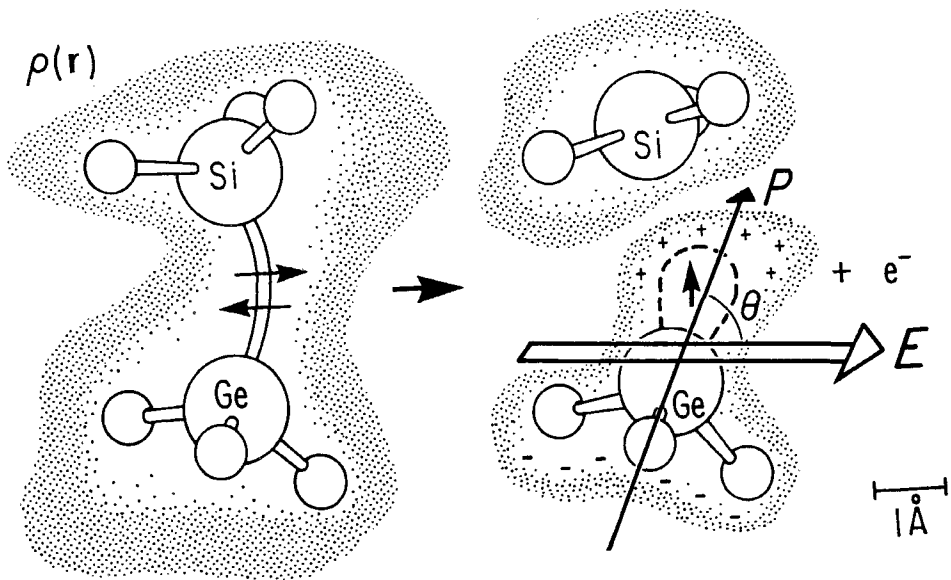


Figure 4 Generic charge distribution around a germanium-silicon-oxygen complex

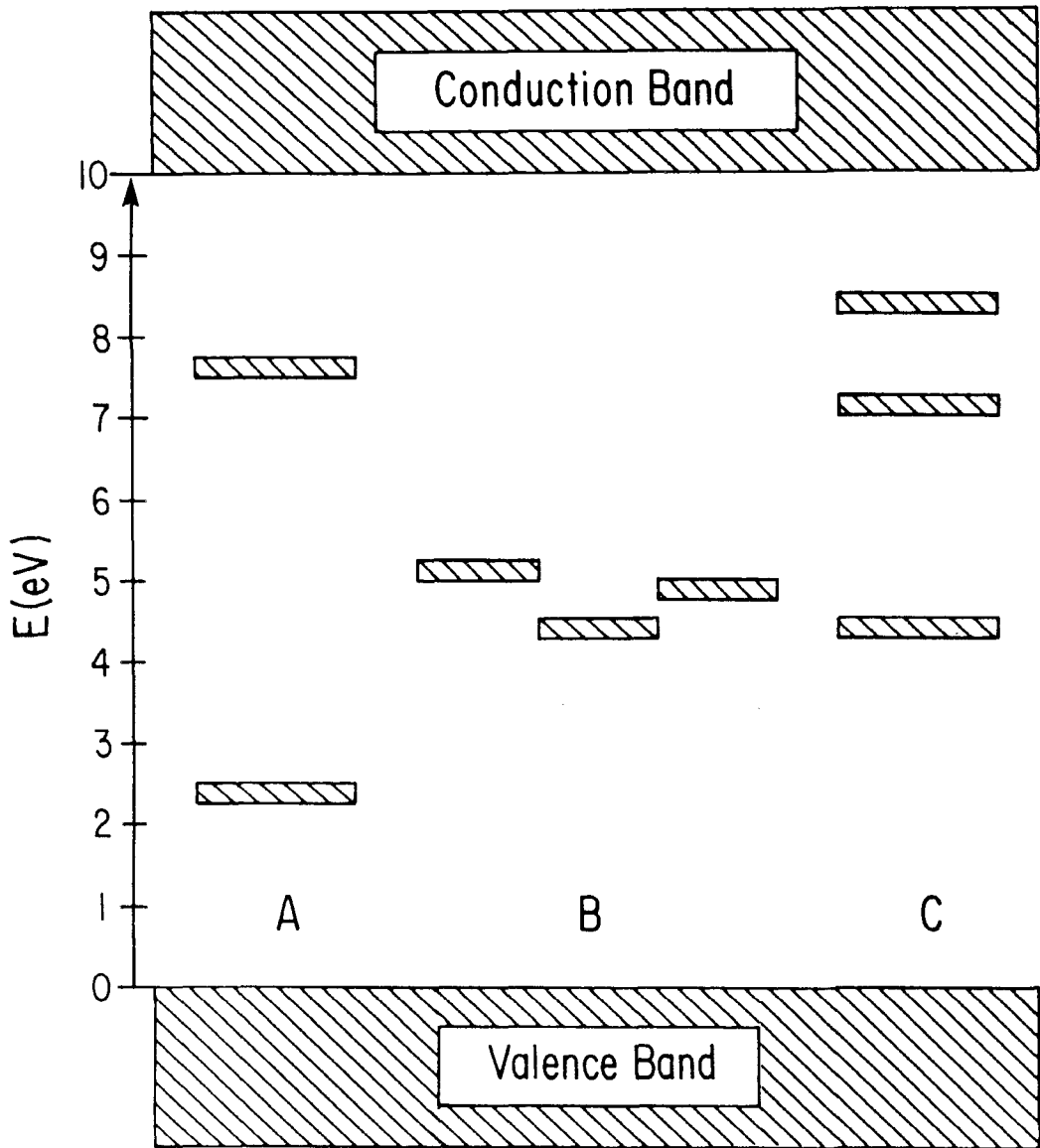
Possible Defect States in Ge-doped α -SiO₂

Figure 5 Proposed energy diagrams for germanosilicate glass

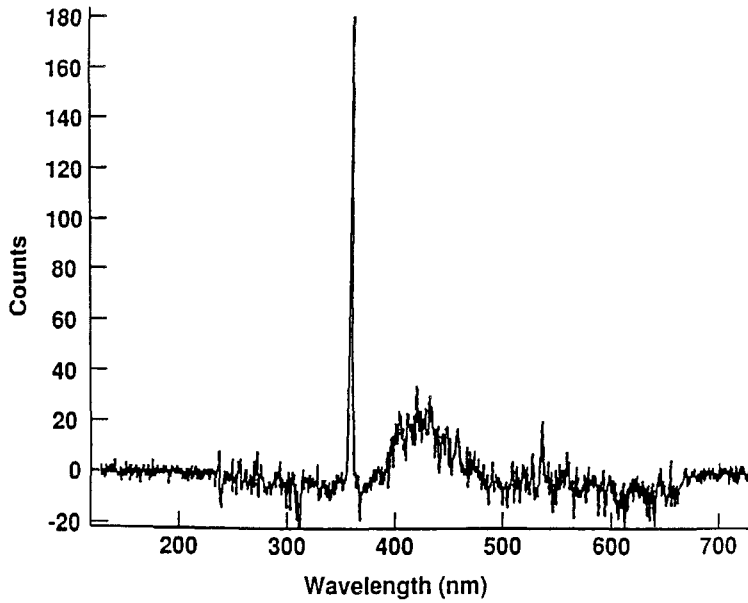


Figure 6 Spectrum after ~ 15 cm long piece of fiber illuminated with light at $\lambda = 1.06 \mu\text{m}$

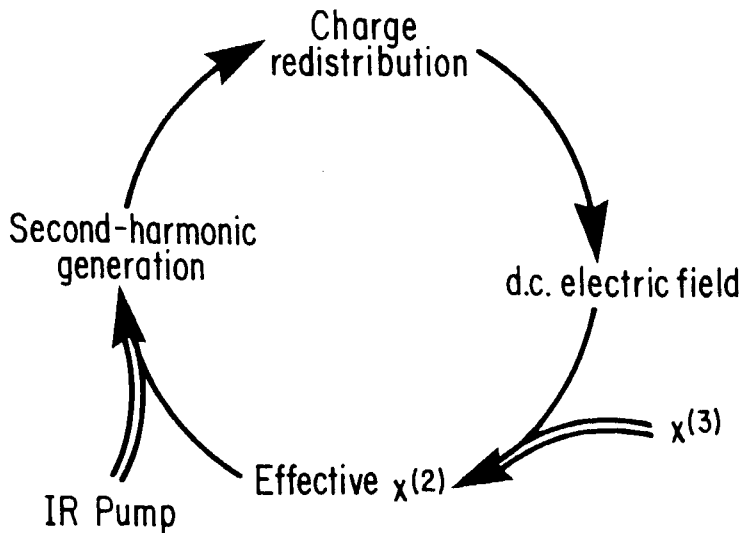


Figure 7 Self-consistency of SHG (courtesy Prof. Dana Anderson, University of Colorado)